Practical Design Considerations and Performance Characteristics of High Numerical Aperture Holographic Lenses

Raymond K. Kostuk

Electrical and Computer Engineering Department, and Optical Sciences Center, University of Arizona Tucson, AZ. 85721, USA

ABSTRACT

The diffraction efficiency of interferometrically formed holographic lenses is influenced by the recording geometry and properties of the recording material. Variations in efficiency increase when attempting to make high numerical aperture elements. In this presentation the factors which influence the diffraction efficiency of high numerical aperture holographic lenses are examined.

1. Introduction

Many factors influence the diffraction efficiency of holographic lenses. These include changes in the visibility of interfering fields across the hologram aperture due to intensity and polarization variations, changes in the average refractive index and thickness of the recording material between exposure and processing steps, and variation of the interbeam angle over the aperture of the hologram. Considering high efficiency phase gratings, these effects physically alter the refractive index modulation at different locations across the aperture.

In order to analyze the influence of these factors, high numerical aperture (0.54 N.A.) holographic objectives were formed in bleached silver halide emulsions using a reversal bleach process. The total efficiency of this lens was 43% compared to a planar grating efficiency of 47% formed with two collimated beams and similar geometrical conditions. The efficiencies of higher diffraction orders for both s- and p- polarized reconstruction beams are mapped across the aperture, and related to the interbeam angles of the construction beams at different locations. Although several evaluations of high N.A. lenses have previously been made[1-3], these investigations only considered a section of the lens containing the grating vector (**K**) which was illuminated with light polarized perpendicular to this plane. This paper provides experimental results for the efficiency of the grating with different **K** vector and reconstruction field polarization orientations.

2. Characterization of Holograms formed in Bleached Silver Halide Emulsions

Holograms for this evaluation were formed in Agfa 8E75HD silver halide emulsions exposed with 632.8 nm illumination, and processed with an Ilford reversal chemistry (SP678C developer/SP679C bleach). This material was chosen because its properties have been well characterized, and because processing is relatively simple and provides consistent results.

Although the efficiency is less than that obtained for dichromated gelatin and some photopolymers, many of the same factors affecting silver halide holograms will also appear in gratings formed in other materials.

The efficiency as a function of exposure for a series of unslanted and slanted planar gratings processed with the reversal chemistry are shown in Figures 1 and 2. (The diffraction efficiency for this analysis is equal to the power in a particular order divided by the incident power.) An interbeam angle of 40° was used for both cases, and the slanted grating formed with one beam at normal incidence to the emulsion and the second at 40° to the normal in air. (This geometry corresponds to the interfering rays at the center of the focusing holographic lens.) Maximum efficiency for the unslanted grating occurs when the hologram is illuminated at the construction angle. However, for the slanted grating, the maximum diffraction efficiency occurs at a different angle from that used during construction. Figure 2 shows that their is about a 10% change in absolute diffraction efficiency (20% relative) near the optimum exposure for this process. This results from changes in the emulsion thickness which effectively rotates the grating plane, and a change in the average refractive index further detunes the grating from peak efficiency at the construction angle. A reversal bleach removes the exposed silver halide crystals which were converted to silver during development[4]. This mechanism reduces both the emulsion thickness and average refractive index producing a drop in efficiency. This same mechanism however, also reduces the negative effects of scatter and noise gratings, and gives reasonably high diffraction efficiency. Since the thickness and average refractive index change could be quantified, the reversal bleach process was used for this evaluation. Measurement of an emulsion exposed with 115 $\mu J/cm^2$ showed an average refractive index change from 1.64 to 1.60, and a thickness reduction from 5.0 μm to 4.5 μm.

3. Factors Affecting the Efficiency of Focusing HOEs

Consider the construction geometry for a holographic lens shown in Fig. 3. In this arrangement an on-axis spherical beam interferes with an off-axis collimated reference beam. The polarization of the reference field is along the y-axis. The spherical beam is formed by focusing collimated beam with its field polarized along the y-axis. The polarization of this beam has a different orientation for each ray illuminating the aperture. Therefore, as the NA of the element increases there will be a larger difference between the polarization vectors of the spherical and reference beams. High numerical aperture elements accentuate this difference and make it necessary to consider vector effects both during construction and reconstrucion.

The configuration of Figure 3 provides a relatively large interbeam angle over much of the grating aperture. This reduces the grating period, increases the overall efficiency, and tends to equalize the efficiency of s- and p- diffracted light[5]. Another advantage of this arrangement is that non-diffracted light in the zero order does not overlap with the focusing beam during reconstruction which would reduce the signal-to-noise level in the region of focus. In addition, the off-axis geometry can also be used to help circularize the reconstruction beam.

In order to analyze the varying efficiency of this hologram a localized planar grating approximation is made at discrete points across the aperture[5]. At the lens center the corresponding planar grating has an interbeam angle of 40° with both fields polarized in the y direction. Plots of the experimental diffraction efficiency vs. reconstruction angle for the central region of a 0.54 NA focusing element and for a hologram formed with two collimated fields are illustrated in Figures 4 and 5 respectively. These holograms were made using the same exposing and processing conditions and show reasonably good correspondence in maximum efficiency, however there is an angular displacement indicating that the probe beam diameter(1mm) may have exceeded the limit for the local plane grating approximation.

The efficiency of a volume hologram depends on the visibility of the interfering fields and the exposure level at the film plane. When the emulsion response is linear, this dependence can be approximated[7] by the relation

$$\eta = SE_oV \quad ,$$

where S is a film sensitivity factor, E_o is the average film exposure, and V is the visibility of the interfering fields within the emulsion. The film sensitivity factor will depend on the particular type of emulsion and processing chemistry. The exposure will vary across the aperture of the focusing element due to changes in the path lengths between the center and edge of the aperture for the expanding spherical beam, and changes in the fresnel coefficients. These differences affect the beam ratio (R) which in turn influence the visibility since

$$V = \frac{2R^{1/2}cos(\Omega)}{(1+R)} \quad ,$$

with Ω the relative orientation of the polarizations of the interfering fields.

Combining these factors and calculating the ratio of the efficiency at the edge of the hologram aperture relative to the center shows (Fig.6) that the expected fall-off for a 0.55 NA element illuminated with an s-polarized reconstruction beam is about 15%, and 25% with a p-polarized beam.

As stated earlier, these calculations assume that η varies linearly with exposure. This is a good assumption for dichromated gelatin and many photopolymers, however materials such as silver halide tend to saturate after reaching a maximum value (Figure 1). This can be used to advantage by exposing the emulsion beyond the linear range of the film. Since the efficiency does not change rapidly with exposure in this region, variations of η across the aperture can be reduced. (It is assumed that nonlinearities in the refractive index modulation were small since measurements showed that very little power went into higher diffraction orders.)

For a highly linear responding material the slope of the efficiency vs exposure can be reduced by using a thinner emulsion. Exposing the emulsion at level slightly above the first η maximum will then keep the total efficiency high over a relatively large exposure range.

Other factors which influence the diffraction efficiency of high numerical aperture HOEs are differences in emulsion thickness and average refractive index between the exposure and post process phase of hologram recording. The effects of these variations on the diffraction efficiency for the slanted planar grating described earlier corresponding to the local grating at the center of the focusing HOE were determined using coupled wave analysis[8] and are illustrated in Figures 7 and 8. As indicated a change in emulsion thickness produces significant displacement and reduction in the efficiency, however a change in the average refractive index of 0.06 results in only a small displacement of the curve (i.e. 2°). Values for the average refractive index and thickness change for emulsions processed with the reversal bleach presented in the previous section indicate that the change in average refractive index is not significant, however the thickness change will produce a major shift in the efficiency performance.

The numerical values in Figure 3 show the normalized coordinates in the x direction and the corresponding interbeam angles $\Delta\theta_{inter}$ for a 0.55 NA lens. These angles can then be used to compute the appropriate grating vector and diffraction efficiency for local planar gratings. For emulsions on the order of 5 μm thick, average refractive index of 1.6, and index modulation of 0.05, the volume grating conditions will not be satisfied across the aperture. This will give rise to higher diffraction orders which extract power from the desired order.

4. Fabrication and Evaluation of High N.A. Holographic Lenses

Holographic lenses were formed with a spherical beam produced with a 0.55 N.A. long working distance microscope objective and a collimated reference beam at 40° to the surface normal of the emulsion. A beam ratio of 1 at the center of the exposed area was obtained by placing a mask with a small diameter aperture in the film plane and then measuring the power in each beam. The film was then exposed with 115 $\mu J/cm^2$ of 632.8nm illumination from a HeNe laser as mentioned in Section 1, and processed with a standard Ilford reversal chemistry. This exposure level was beyond the linear range of the film/process combination (Figure 1), and was expected to improve uniformity in the efficiency over the aperture of the HOE.

After processing the hologram was illuminated with the conjugate of the planar reference beam. A mask with a 1 mm aperture was mounted on an x-y translational stage to probe the efficiency at different locations in the aperture. Both s- and p- polarized light was used to illuminate discrete positions along the x- and y-axes of the hologram. The results of these measurements are shown in Figures 9-12. The smallest interbeam angle exists at the x = -1.0 positions on the x-axis efficiency plots. The +1 and -1 diffraction orders are equal at this coordinate indicating that the grating acts like a thin sinusoidal grating. There are several weaker diffraction orders (R_o, T(-2), and R(-1)) not shown on these figures for clarity which account for an additional 15% of the incident illumination at the x = -1 position. In each case the efficiency of the primary order also decreases near the edge of the aperture with the largest interbeam angle. It is not exactly clear if this drop is a result of a decrease in exposure or is due to an overcoupling effect. From Figures 1 and 2 it can be seen that a slanted grating does not saturate in the same manner as an unslanted

one. This effect would be accentuated near the edge of the hologram aperture where the interbeam angle in air is close to 73°. Given these limitations however, the total s- and p-efficiencies over the complete aperture were 43.1 and 41.7% respectively. A corresponding planar grating formed with a normally incident beam and a second beam at 40° to the emulsion normal had an s-polarized reconstruction beam efficiency of 47%. Using this as a reference for the maximum efficiency obtainable with this film and process chemistry, the focusing element efficiency is approximately 92% of the possible planar grating efficiency.

Acknowledgements

The author wishes to acknowledge support for this work from IBM, the University of Arizona Optical Data Storage Center, and NSF contract # ECS-8910067.

5. References

1. C. Kojima, K. Miyahara, K. Hasegawa, T. Otobe, and H. Ooki, "In-Line Holographic Lenses of High Numerical Aperture," Japan. J. Appl. Phys., 20, Supplement 20-1, 199-204 (1980).
2. R.R.A. Syms and L. Solymar, "Higher diffraction orders in on-axis holographic lenses," Appl. Opt., 21, 3263-3268 (1982).
3. R.R.A. Syms and L. Solymar,"Experimental and theoretical evaluation of the efficiency of an off-axis volume holographic lens," Appl. Phys. B 32, 165-173 (1983).
4. G. Saxby, Practical Holography, Prentice Hall, p.73, (1988).
5. A.B. O'Connor and R.K. Kostuk, "Polarization properties of high numerical aperture holographic objectives," OSA Topical Meeting on Optical Data Storage, Los Angeles, CA. 17-19 Jan. 1989, Technical Digest p.95-97.
6. R.R.A. Syms and L. Solymar,"Localized one-dimensional theory for volume holograms," Opt. Quant. Electron., Vol. 13, 415-419 (1981).
7. L.H. Lin, "Method of characterizing hologram-recording materials," J.Opt. Soc. Am., Vol. 61, 203-208 (1971).
8. H. Kogelnik, "Coupled wave theory for thick hologram gratings," Bell Syst. Tech. J., Vol. 48, 2909-2947 (1969).

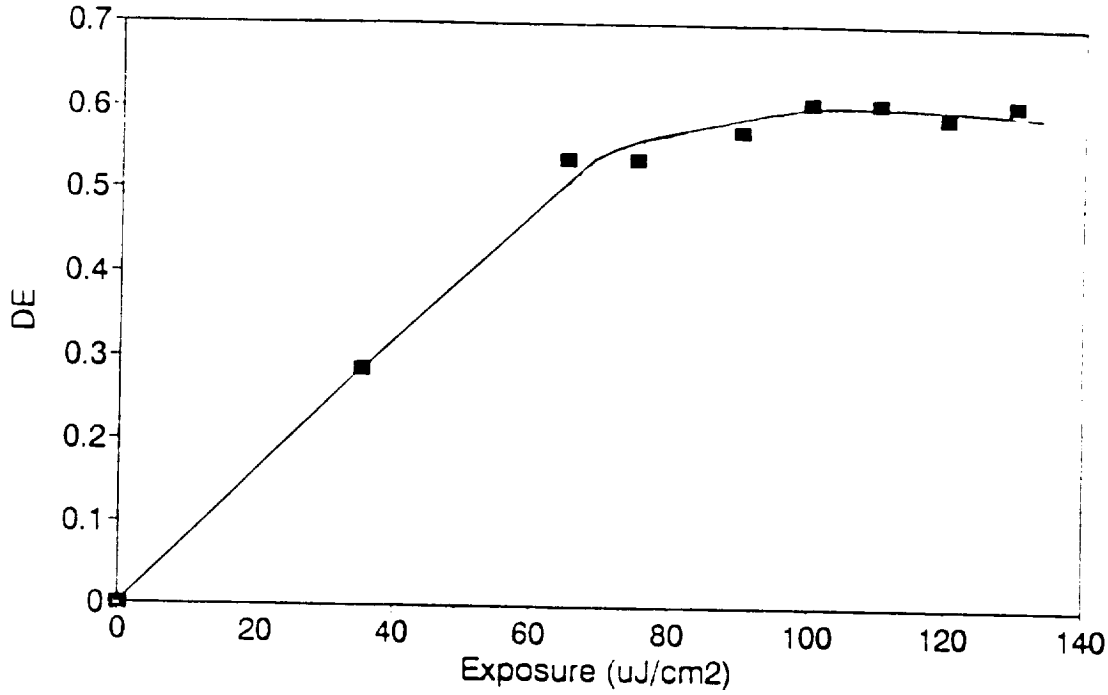

Figure 1. Diffraction efficiency vs. exposure for Agfa 8E75HD emulsions processed with Ilford SP678C developer and SP679C reversal bleach. Grating planes are normal to the emulsion surface, and was formed with two collimated beams having a 40° interbeam angle in air.

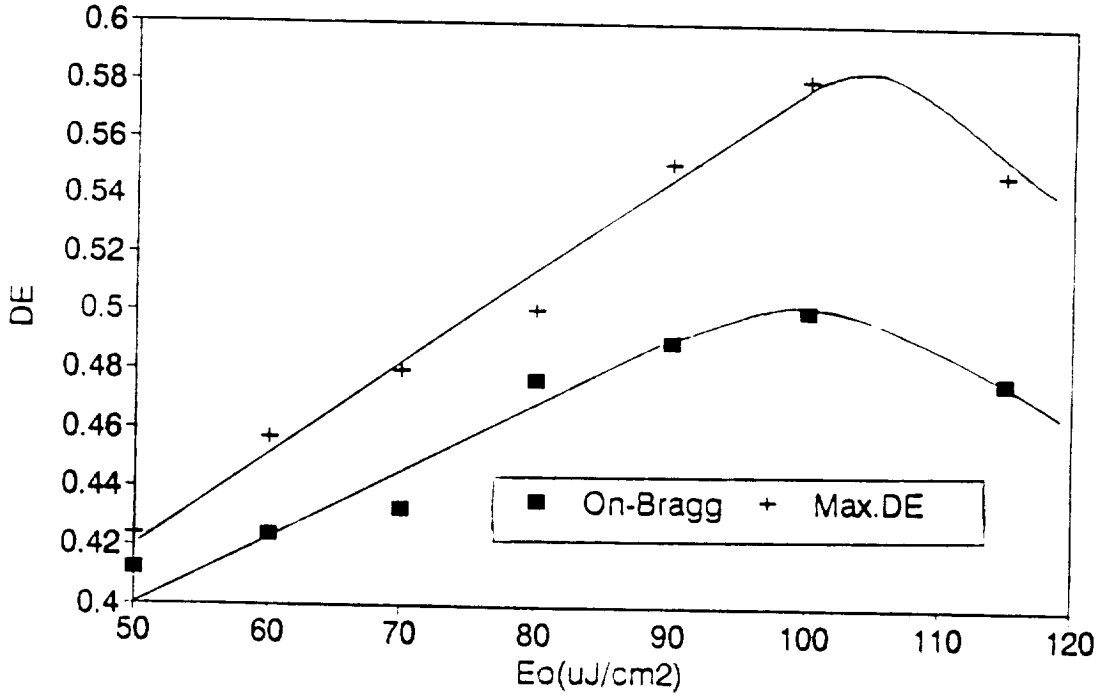

Figure 2. Diffraction efficiency vs. exposure for a planar grating formed in Agfa 8E75HD emulsions processed with Ilford SP678C developer and SP679C bleach. The slanted grating was formed with one beam normal to the emulsion surface and the second at 40° to the normal in air. The upper curve shows maximum efficiency obtained by rotating the grating, and the second is reconstructed at the formation angle.

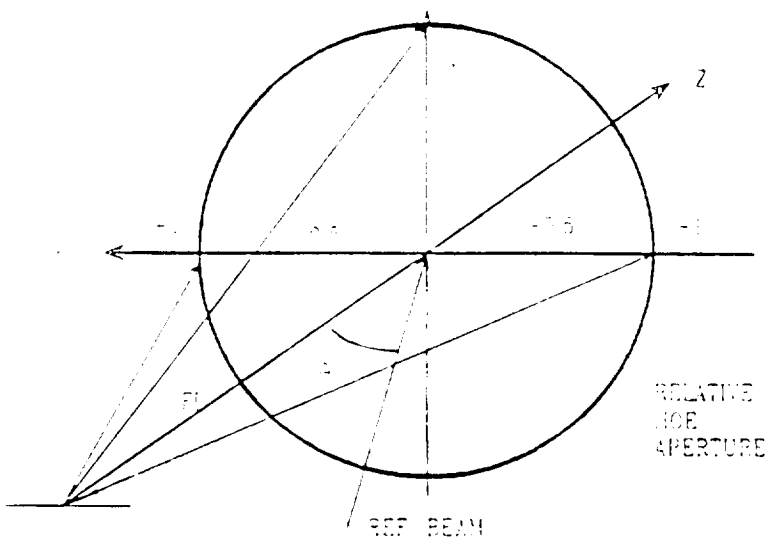

X/(D/2)	Δθ
-1.00	
-0.75	14.3°
-0.5	22.2°
-0.25	30.9°
0.00	40.0°
0.25	49.1°
0.50	57.8°
0.75	65.7°
1.00	72.7°

Figure 3. Construction geometry for a high N.A. lens formed with an on-axis spherical and an off-axis collimated reference wave. Also shown are different interbeam angles (in air) which exist along the x-axis.

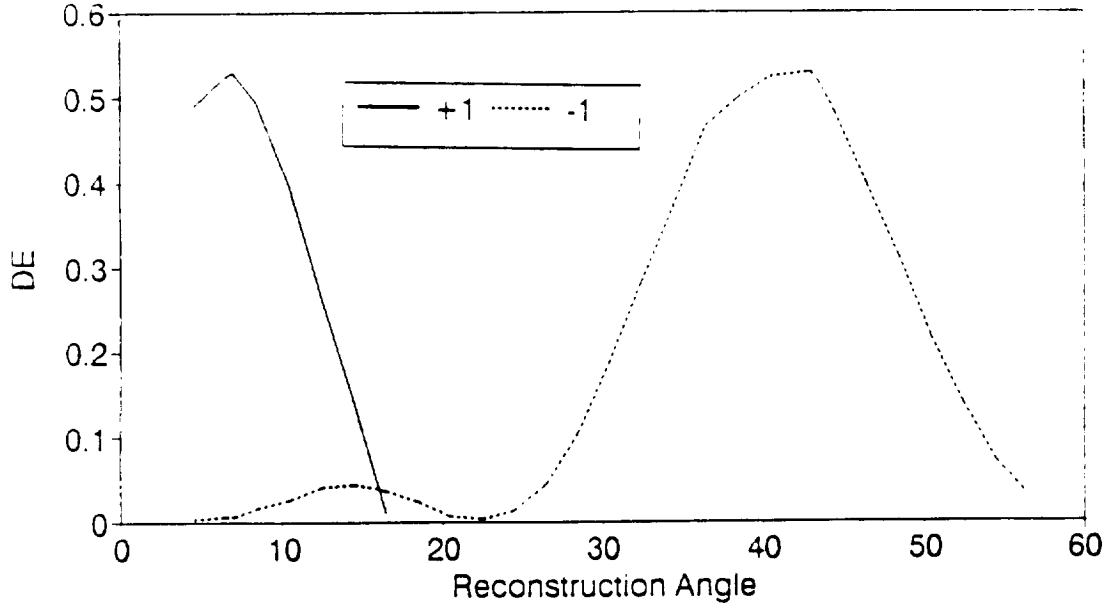

Figure 4. Diffraction efficiency vs. reconstruction angle at the center of the 0.54 N.A. focusing HOE.

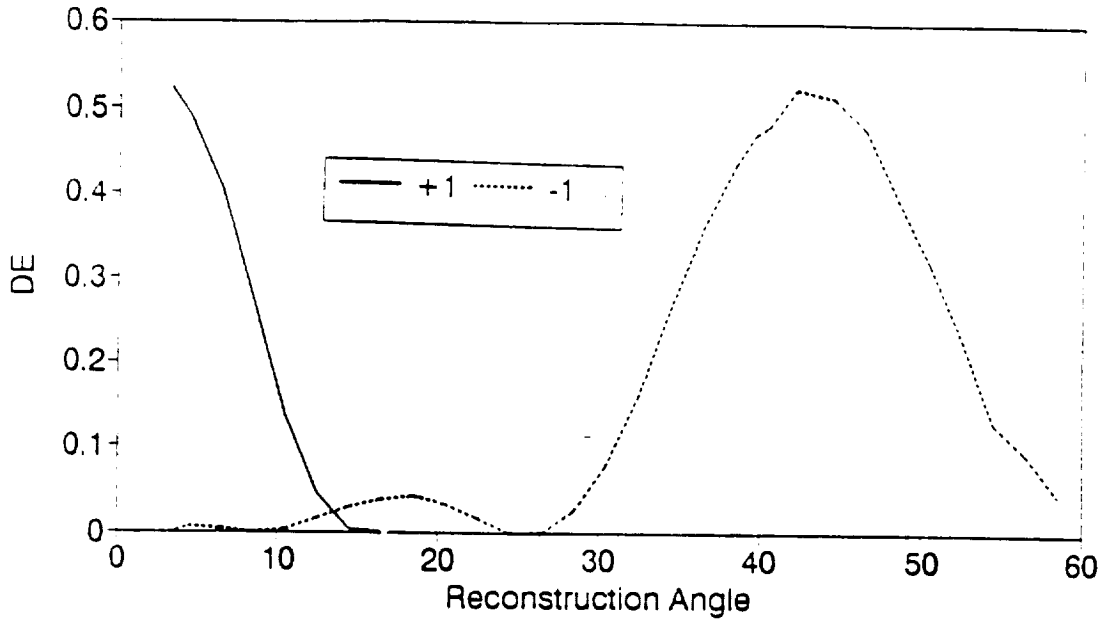

Figure 5. Diffraction efficiency vs. reconstruction angle for a planar grating corresponding to the local planar grating at the center of the 0.54 N.A. focusing HOE.

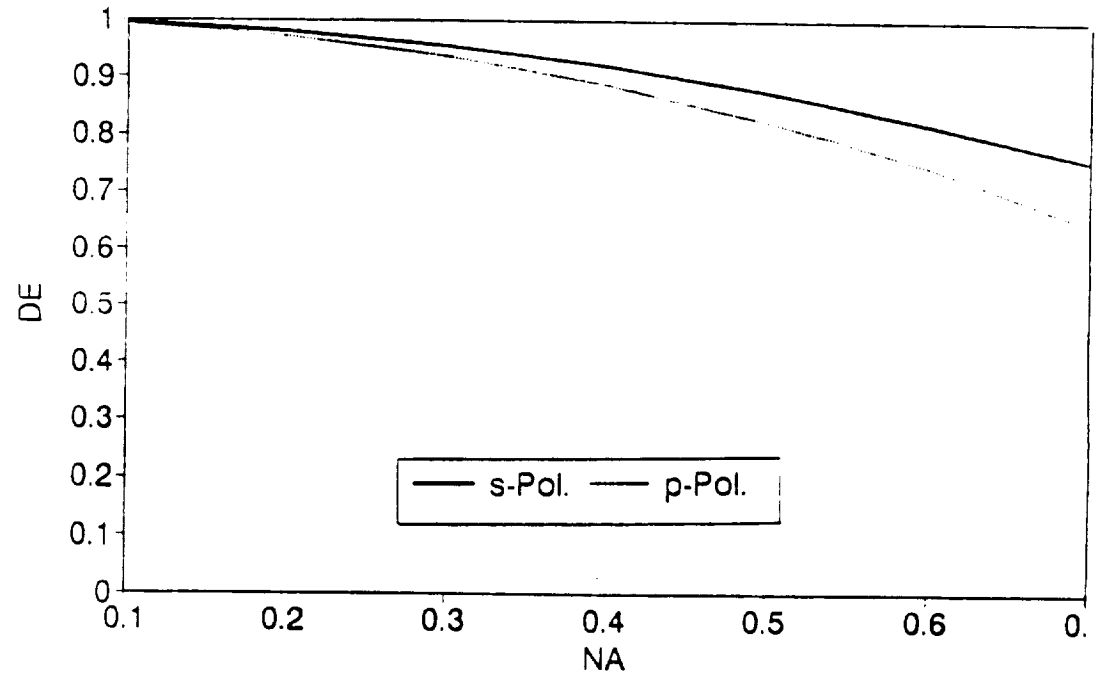

Figure 6. Drop in diffraction efficiency with N.A. resulting from exposure variation, polarization mismatch, and different Fresnel coefficients across the aperture. A linear dependence on exposure and visibility is assumed.

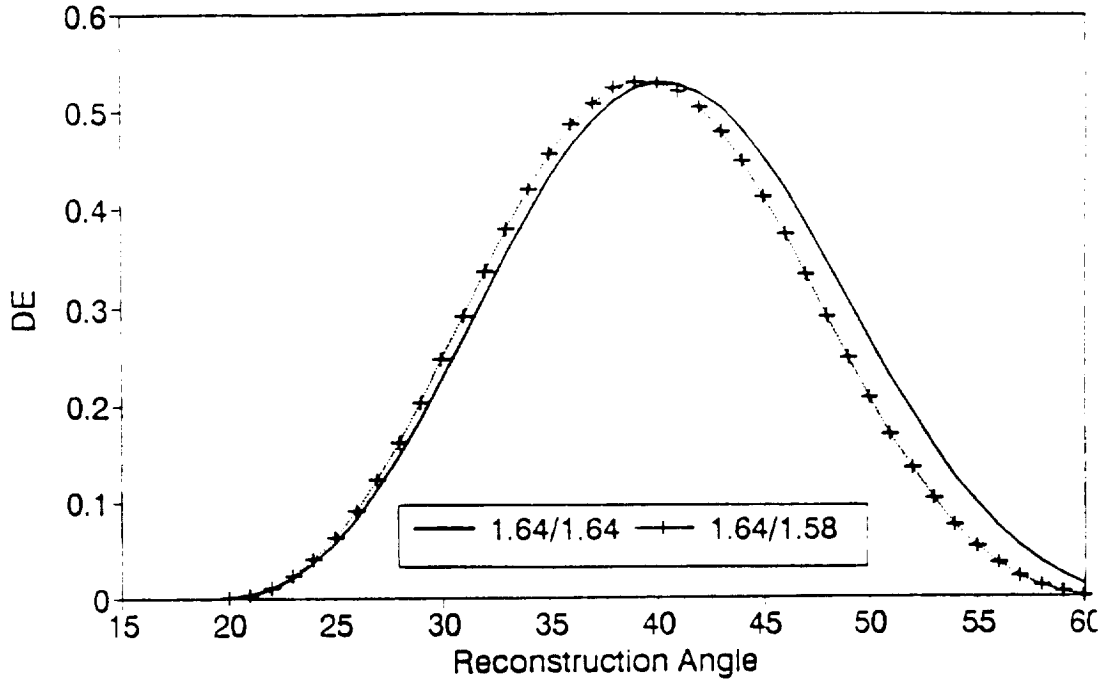

Figure 7. Diffraction efficiency vs. reconstruction angle for a planar grating formed and reconstructed with the same average refractive index, and with a change of 0.06 in index.

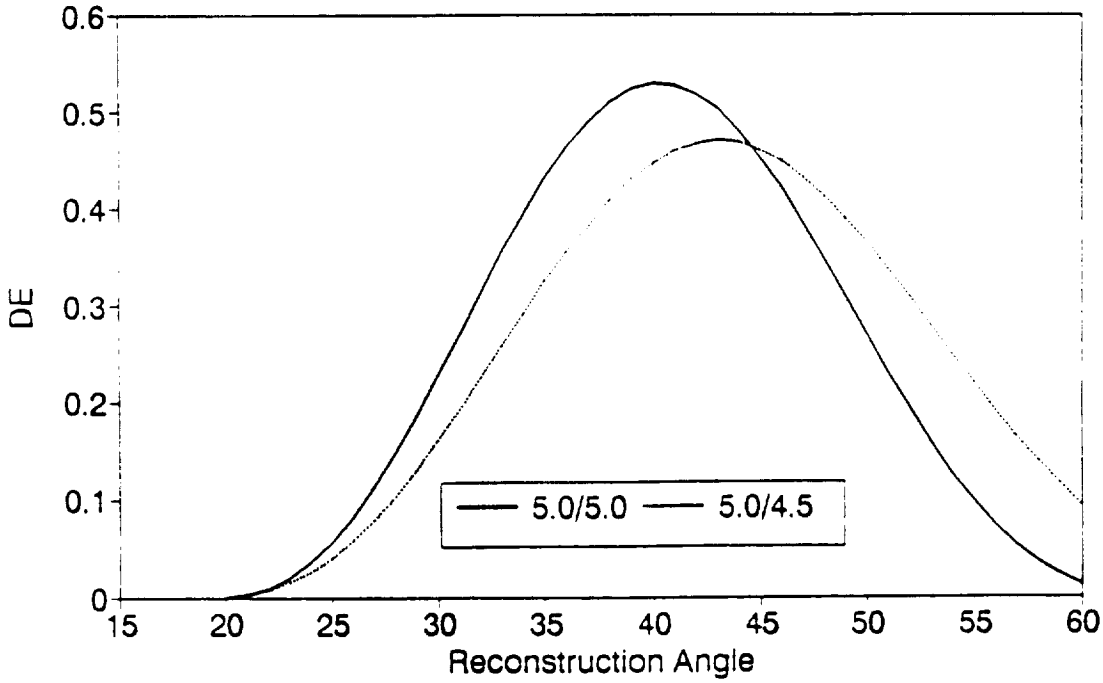

Figure 8. Diffraction efficiency vs. reconstruction angle for a planar grating formed and reconstructed with the same average refractive index, and with a change of 0.06 in index.

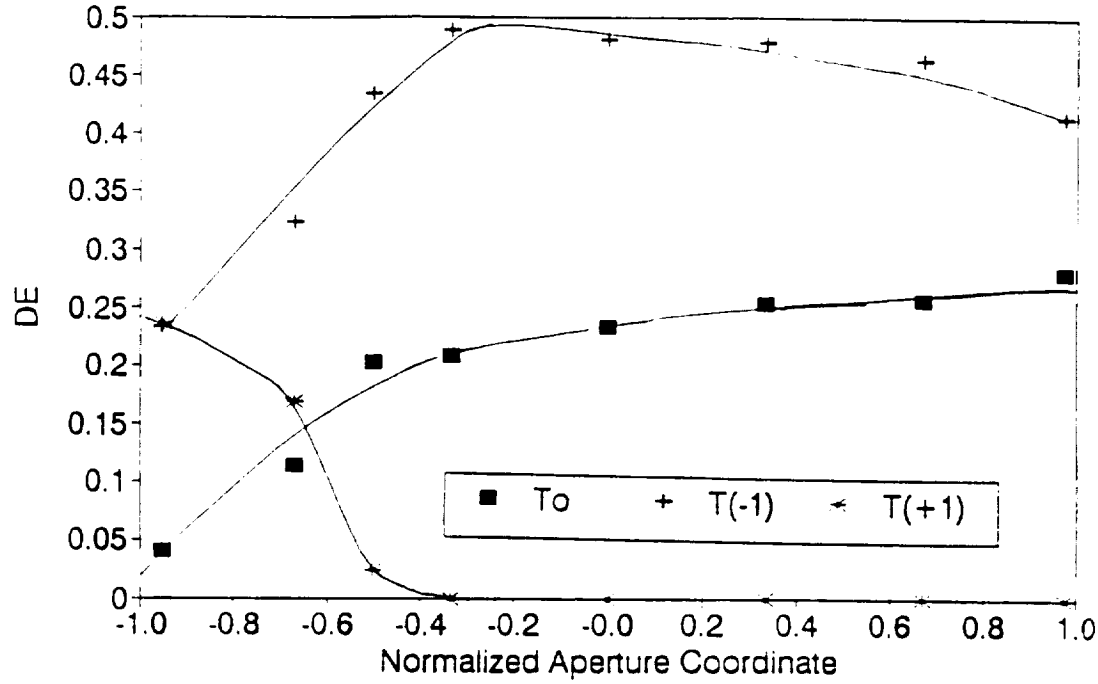

Figure 9. Measured diffraction efficiency across the x-axis of a 0.54 N.A. HOE reconstructed with s-polarized light.

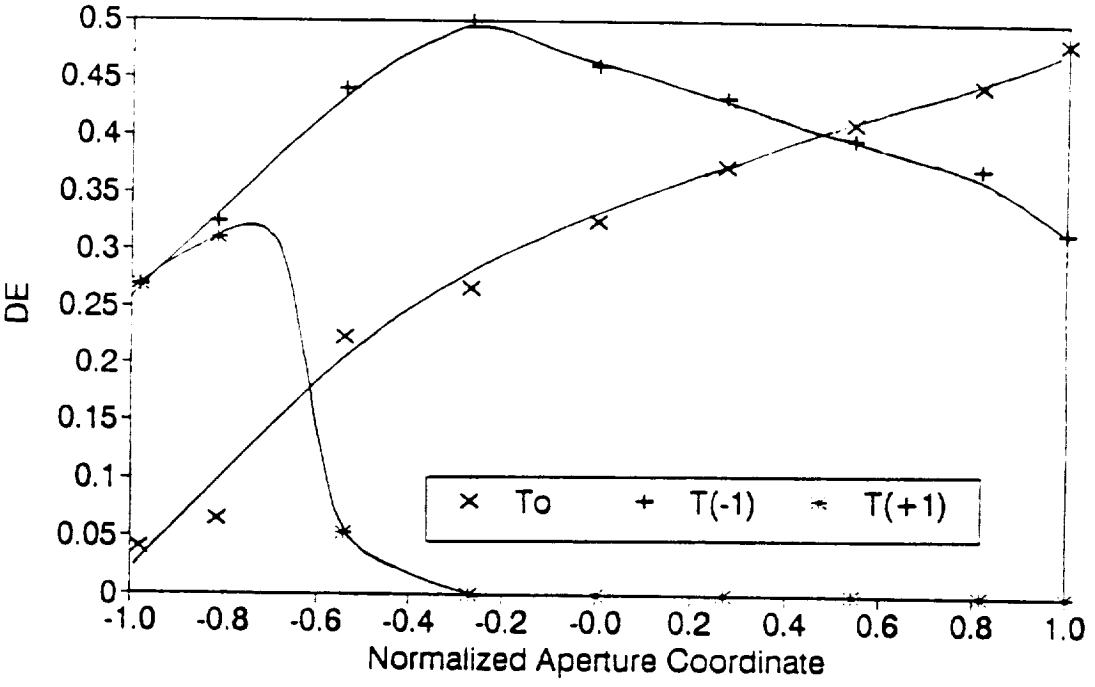

Figure 10. Measured diffraction efficiency across the x-axis of a 0.54 N.A. HOE reconstructed with p-polarized light.

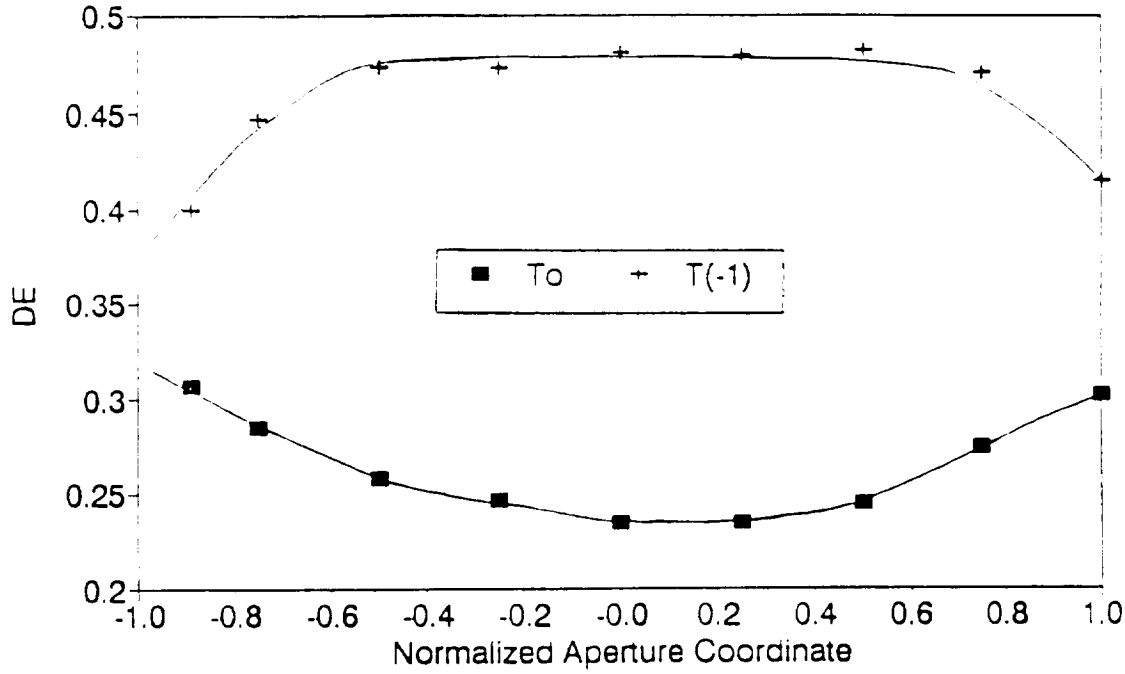

Figure 11. Measured diffraction efficiency across the y-axis of a 0.54 N.A. HOE reconstructed with s-polarized light.

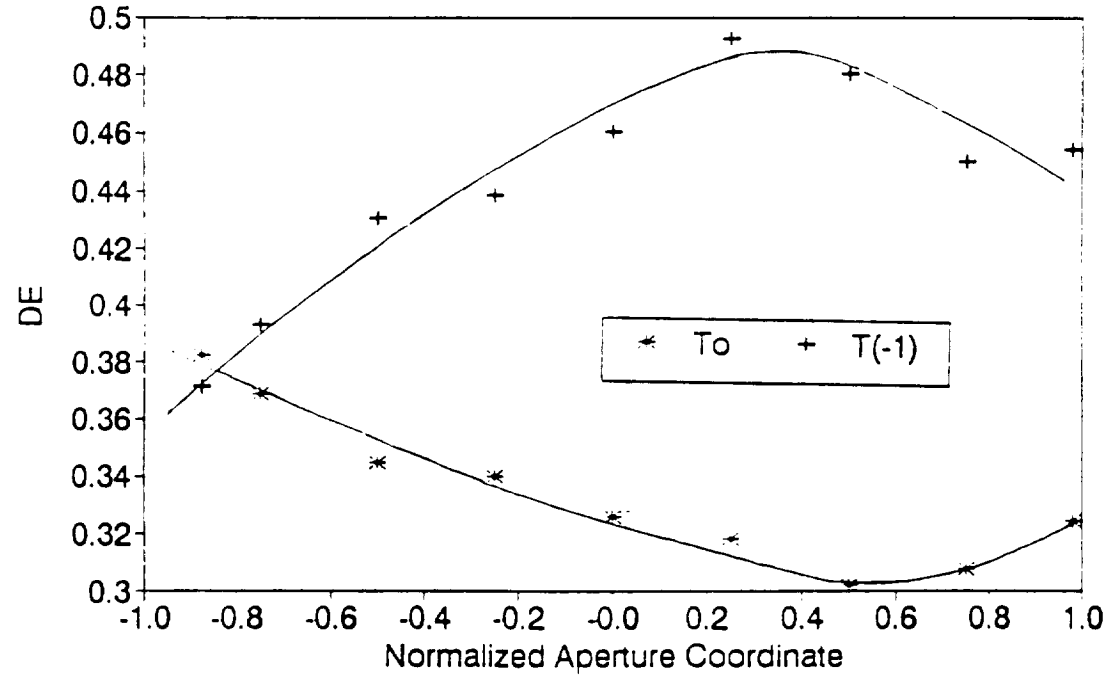

Figure 12. Measured diffraction efficiency across the y-axis of a 0.54 N.A. HOE reconstructed with s-polarized light.